Functional Flow Cytometry to predict PD-L1 Conformational Changes

Roser Salvia[1#], Laura G. Rico[1#], Mike D. Ward[2], Jolene A. Bradford[2], and Jordi Petriz[1*]

[1] Functional Cytomics Lab, Germans Trias i Pujol Research Institute (IGTP), ICO-Hospital Germans Trias i Pujol, Universitat Autònoma de Barcelona, Badalona (Barcelona), Spain.

[2] Thermo Fisher Scientific, Eugene, Oregon, USA.

# Those two authors contributed equally to this chapter

* Corresponding Author: Jordi Petriz, PhD

Contact information:

Roser Salvia, MSc: Germans Trias i Pujol Research Institute (IGTP), Crta. de Can Ruti, Camí de les Escoles s/n, Edifici Mar, 08916 Badalona (Barcelona), Spain; e-mail: rsalvia@igtp.cat

Laura G. Rico, PhD: Germans Trias i Pujol Research Institute (IGTP), Crta. de Can Ruti, Camí de les Escoles s/n, Edifici Mar, 08916 Badalona (Barcelona), Spain; e-mail: lgarcia@cytognos.com

Michael D. Ward, PhD: Thermo Fisher Scientific, 145 E. Mountain Rd, Ft Collins, CO, 80524, USA; e-mail: mike.ward@thermofisher.com

Jolene A. Bradford, PhD: Thermo Fisher Scientific, 29851 Willow Creek Rd Bldg J, Eugene, OR, 97402, USA; e-mail: Jolene.bradford@thermofisher.com

Jordi Petriz, PhD: Germans Trias i Pujol Research Institute (IGTP), Crta. de Can Ruti, Camí de les Escoles s/n, Edifici Mar, 08916 Badalona (Barcelona), Spain; e-mail: jpetriz@igtp.cat

ABSTRACT:

The Programmed Cell Death Protein 1/Programmed Cell Death Protein Ligand 1 (PD-1/PD-L1) axis is one of the most widely recognized targets for cancer immunotherapy. Importantly, PD-L1 conformational changes can hinder target binding when living cells are used. Antibody affinity, equilibrium binding, association and dissociation rates, and other affinity related constants are fundamental to ensure target saturation. PD-L1 changes in conformation are explored here, with potential impact on PD-L1 function and mutation. We present detailed flow cytometry procedures to analyze PD-L1 reactivity in Myeloid-Derived Suppressor Cells (MDSCs). This approach can also be used to study the contribution of protein conformational changes in living cells.

Basic Protocol 1: Sample preparation for PD-L1$^+$ Myeloid-Derived Suppressor Cells detection by flow cytometry
Basic Protocol 2: Protocol preparation, sample acquisition and gating strategy for flow cytometric screening of PD-L1$^+$ Myeloid-Derived Suppressor Cells in lung cancer patients
Support Protocol 1: Bioinformatic tools for the analysis of flow cytometric data

KEYWORDS:

PD-L1; Flow Cytometry; Immunotherapy; MDSC; NSCLC

INTRODUCTION:

PD-L1 expression levels in tumor and immune cells are used as a predictor of response to immunotherapy in several tumor types (Patel & Kurzrock, 2015). PD-L1 assessment is currently performed by immunohistochemistry (IHC) assays and is associated with increased efficacy of immune-checkpoint inhibitors used in therapy (Paver et al., 2021; Scheel & Schäfer, 2018). Nevertheless, PD-L1 protein expression appears to be heterogeneous (Yue et al., 2018) and can be associated with contradictory clinical outcomes (Borghaei et al., 2020; Brahmer et al., 2015; Ding et al., 2022; McLaughlin et al., 2016). The PD-L1 molecule has been described to have conformational flexibility of 38° within the V and C domains of free and complexed PD-L1, in specific flexible regions such as C"D loop and BC loop as well as Met115, which is postulated to occur for a better interaction to PD-1 (Ahmed & Barakat, 2017; Lin et al., 2008). Moreover, the PD-1 molecule is also reported to have structural flexibility in the CC' loop of the apo-protein for the open and closed conformations, consisting in a 90° twist and 5 Å displacement of Cα carbons (Zak et al., 2015).

Many other molecules have been described to present conformational changes in their structure, such as the human serum transferrin (Campos-Escamilla et al., 2021) or G protein-coupled receptors (Duan et al., 2021; Latorraca et al., 2017). This conformation dynamics can affect the binding of antibodies, as illustrated in the following examples. The ATP-dependent efflux pump P-glycoprotein (P-gp) is known to present conformational changes associated to different stages of transport-associated ATP hydrolysis, promoting drug movement along the translocation pathway. Interestingly, the anti-P-gp UIC2 antibody shows differential reactivity to P-gp depending on their distinct conformations (Mechetner et al., 1997; Vahedi et al., 2018). Furthermore, Tino et colleagues described prostate-specific membrane antigen (PSMA)-specific antibodies that bind exclusively to particular protein conformational epitopes (Tino et al., 2000). Regarding glypican-3 (GPC3), the HN3 antibody binds to a unique conformational epitope of this GPC3 protein, inhibiting cell growth in several hepatocellular carcinoma cell models (Feng et al., 2013). Additionally, antigen glycosylation is another aspect to consider in relation to antibody reactivity, since carbohydrates may mask some peptide epitopes and therefore reduce the antibody binding efficiency (Sotillo et al., 2014).

A well-known strategy for the study of conformational dynamics is the Förster resonance energy transfer (FRET) phenomena. The use of confocal microscopy to assess FRET is widespread because of their subcellular resolution, time-course measurements and morphology-based cell discrimination. On the other hand, flow cytometric analysis of FRET offers a rapid determination of the fluoresce intensity distribution in a population, and notably in spectral flow cytometry, the unmixing of spectral fingerprints permits real-time precise and sensitive discrimination between cells with distinct FRET levels (Henderson et al., 2022; Szabó et al., 2022). Unfortunately, in this situation the currently available monoclonal antibodies cannot detect the PD-L1 epitope of MDSC, and only upon stimulation can the antibodies access to the epitope. Nevertheless, if new monoclonal antibodies are able to target the PD-L1 epitope of MDSC on a basal condition, the conformational change may then be studied with FRET.

The use of tumor biopsies is in general an important limitation for research studies, based on the small size of the tissue obtained. Interestingly, though, the study of peripheral blood also gives an indication of clinical status and resistance to immunotherapy. In fact, Myeloid-Derived Suppressor Cells (MDSCs) are associated with poor prognosis in patients with solid tumors, as in the case of Non-Small Cell Lung Cancer (NSCLC) (Koh et al., 2020; Yamauchi et al., 2018; Zhang et al., 2016), and are crucial in controlling and maintaining the tumor microenvironment (Marvel & Gabrilovich, 2015). Indeed, another strategy to assess PD-L1 consists of a less-invasive method of monitoring the circulating MDSCs from peripheral blood, based on their immunophenotype $CD11b^{+}CD33^{+}HLA\text{-}DR^{low/-}$ (Gabrilovich & Nagaraj, 2009; Hoechst et al., 2008) using flow cytometry. In this chapter, the authors fully describe a flow cytometric protocol for PD-L1 screening in circulating MDSCs. This method follows minimal sample perturbation strategies (Petriz et al., 2018; Rico, Salvia, et al., 2021), avoiding lysing and centrifugations steps and using viable permeant DNA-fluorescent stains to discriminate leukocytes from non-nucleated cells and background. A key step of this protocol is that cells are stimulated in the presence of Phorbol 12-Myristate 13-Acetate (PMA), which results in a dramatic increase of PD-L1 reactivity.

The performance of this flow cytometric protocol enables the assessment of PD-L1 expression in circulating MDSCs, which can be associated with the disease state and used as a predictor of immune checkpoint inhibitor therapy success. For global analysis, the authors take advantage of bioinformatic algorithms such as t-SNE, UMAP and FlowSOM to display the data according to potential similarities from cluster analysis. This minimally invasive method represents a rapid assessment of PD-L1, which seeks to preserve the native structure of the molecule. The presented methodology can be used as a complementary adjunct to current immunohistochemistry assays.

Basic protocol 1 indicates in detail how to prepare peripheral blood samples for immunophenotyping on these immune cells following a minimal sample perturbation protocol. Immunophenotyping of MDSCs and PD-L1 is performed after a stimulatory assay described in this protocol. Basic Protocol 2 describes flow cytometry procedures (flow cytometer setup, instrument and

sample acquisition settings, and gating strategy) for the identification of PD-L1 in MDSCs. Finally, Support Protocol 2 describes the analysis of the obtained data by using software tools for dimensionality reduction.

BASIC PROTOCOL 1:

Sample preparation for PD-L1+ Myeloid-Derived Suppressor Cells detection by flow cytometry

This protocol describes the preparation of peripheral blood samples for flow cytometry screening of PD-L1 in MDSCs. Peripheral blood samples were obtained from healthy donors and lung cancer patients receiving immunotherapy with immune checkpoint inhibitors α-PD-1 or α-PD-L1. The protocol design allows the identification of the leukocyte compartment in peripheral whole blood and the analysis of MDSCs based on their immunophenotyping. It follows a minimal sample perturbation methodology to avoid potential changes in PD-L1 conformation. Incubation with PMA will trigger the unfolding of PD-L1, resulting in an increased reactivity against the antibody specially used to target this molecule. DMSO, the solvent used for PMA preparation, is used as a negative control, and will not trigger any conformational change and is used as a negative control.

Materials:

Freshly drawn EDTA-anticoagulated peripheral whole blood obtained from lung cancer patients
Anhydrous dimethyl sulfoxide (DMSO; Invitrogen™, cat. no. D12345)
Phorbol 12-myristate 13-acetate (PMA; Sigma–Aldrich®, cat. no. P8139-1MG) 1 mg/ml in DMSO (see recipe in Reagents and Solutions)
Hanks' Balanced Salt Solution (calcium- and magnesium-free, without phenol red) with Bovine Serum Albumin and Sodium Azide (HBA; see recipe in Reagents and Solutions)
Türk solution (see recipe in Reagents and Solutions), optional
Vybrant™ DyeCycle™ Violet Stain 5 mM in DMSO (DCV; Invitrogen™, cat. no. A14353)
Fetal Bovine Serum (FBS; Biowest, cat. no. S18B-500)
7-Aminoactinomycin D (7-AAD; Invitrogen™, cat. no. A1310) 1 mg/ml (see recipe in Reagents and Solutions)
PD-L1-PE (Invitrogen™, MIH1, RRID: AB_11042286)
CD11b-APC (Life Technologies™, VIM12, RRID: AB_2536483)
HLA-DR-FITC (Life Technologies™, TU36, RRID: AB_10374000)
CD33-PE-Cy7 (Invitrogen™, WM-53, RRID: AB_1907380)

Water bath, set at 37 °C
Hemocytometer, or other cell counting devices
Micro-centrifuge
EDTA-anticoagulated blood collection tubes
Eppendorf tubes

Protocol steps with step annotations:

Sample preparation

1. Set a circulating bath in a light-protected area at exactly 37 °C.
2. Remove PMA and DMSO from storage and allow them to thaw.
3. Collect freshly drawn whole blood from lung cancer patients in a 3 ml EDTA-anticoagulated tubes.

   Process the collected blood as soon as possible, ideally in less than 4 hours after extraction.

4. Prepare two Eppendorf tubes labeled as DMSO and PMA respectively.
5. Count nucleated cells accurately. Resuspend whole blood in 1 ml HBA to a final concentration of 0.5-1 x 10^6 nucleated cells/ml in each tube by reverse pipetting technique.

   Cells can be counted using either a hematology analyzer or a hemocytometer (Neubauer chamber). For cell counting on a hemocytometer, lyse erythrocytes with Türk solution (see recipe), adding 900 µl of this solution to 100 µl of whole

blood. Incubate diluted sample for 5 min, and place 20 µl of the diluted cells on a hemocytometer. Count nucleated cells at low magnification, preferably using phase-contrast microscopy.

DNA staining and blockading

6. Add 2 µl of DCV 5 mM to a final concentration of 10 µM.
7. Add 10 µl FBS.
8. Homogenize.
9. Incubate 10 minutes at exactly 37 °C in a water-dedicated bath protected from light.

PMA stimulation

10. Add 1 µl DMSO to one Eppendorf and 1 µl PMA to the other.
11. Homogenize.
12. Incubate 5 min at 37 °C protected from light.
13. After incubation, centrifuge both Eppendorf tubes (short spin of about 10 seconds).
14. Remove 900 µl of the supernatant and reserve it.

Antibody staining

15. Add 2.5 µl PD-L1-PE, 2.5 µl HLA-DR-FITC, 2.5 µl CD11b-APC, and 5 µl CD33-PE-Cy7 into both Eppendorf tubes.

    Cover the samples with aluminum foil to minimize the time of light exposure.

16. Homogenize.
17. Incubate 20 min at room temperature protected from light.

    Place the tubes horizontally to facilitate the antibody staining.

Necrotic cells staining

18. Add into both tubes the 900 µl of each reserved supernatant.
19. Add 2 µl 7-AAD 1 mg/ml to a final concentration of 1.5 nM.
20. Resuspend gently and incubate 5 min at room temperature in the dark.

BASIC PROTOCOL 2

Protocol preparation, sample acquisition and gating strategy for flow cytometric screening of PD-L1+ Myeloid-Derived Suppressor Cells in peripheral blood

Flow cytometric screening of PD-L1 in MDSCs using whole blood provides a new complementary approach to current immunohistochemistry assays. Using this assay, the authors analyze PD-L1 expression as the percentage of MDSCs in nucleated cells, by quantifying the mean fluorescence intensity, and by estimating the fold-change status of this molecule when comparing with the unstimulated and stimulated specimens.

The protocol design should help to identify MDSCs based on $CD11b^{+}CD33^{+}HLA\text{-}DR^{low/-}$ reactivity. Monocytic/mononuclear MDSCs (M-MDSCs) are characterized by the expression of CD14, and granulocytic/polymorphonuclear MDSCs (PMN-MDSCs) by the expression of CD15 (Gabrilovich & Nagaraj, 2009). CD14 and CD15 monoclonal antibodies are not used in this protocol as the authors alternatively identify these populations by discriminating $CD33^{+}/CD11b^{hi}$ for M-MDSCs and by $CD33^{hi}/CD11b^{+}$ for PMN-MDSCs. Using this strategy, the authors simplify the protocol to minimize fluorescence spillover issues. The gating strategy identifies nucleated cells based on fluorescent viable DNA stains, and MDSCs based on previously described immunophenotyping to finally study PD-L1 expression in this subpopulation.

Materials:

Cells to be analyzed (see Support Protocol 1)

Flow cytometer equipped with lasers and filters allowing the excitation and detection of all used fluorochromes and absolute cell counting. The authors of this chapter use the Invitrogen™ Attune™ NxT Flow Cytometer.

For blue excitation:

Flow cytometer equipped with blue laser operating at ~488 nm

Filter combinations consisting of 488/10 band-pass (forward scatter, FSC), 530/30 band-pass (green emission), and 695/40 band-pass (red emission)

For violet excitation:

Flow cytometer equipped with violet laser operating at ~405 nm

Filter combinations consisting of 405/10 band-pass (side scatter, SSC) and 440/40 band-pass (blue emission)

For yellow/green excitation:

Flow cytometer equipped with yellow/green laser operating at ~561 nm

Filter combinations consisting of 585/16 band-pass (orange emission) and 780/60 band-pass (infra-red emission)

For red excitation:

Flow cytometer equipped with red laser operating at ~640 nm

Filter combinations consisting of 670/14 band-pass (red emission)

NOTE: For the acquisition of whole blood samples, collecting the side-scatter parameter with violet laser emission is recommended because the height parameter is more accurate for violet SSC than for blue SSC. For more information, please check (Petriz et al., 2018)*. However, if the cytometer configuration does not allow obtaining violet SSC, default SSC signal can alternatively be used.*

Protocol steps with step annotations:

Flow cytometer setup

1. Start up the flow cytometer and allow it to warm up.
2. Check that all the fluids have been refilled.
3. Carry out the performance validation of the flow cytometer with the required fluorescent beads according to the manufacturer's instructions.
4. When available, configure the appropriate filter array to collect the violet side-scatter signal.

Protocol preparation

5. Create a density/dot plot displaying SSC-H on a linear scale versus DCV-H on a logarithmic scale and gate all live DNA-positive cells, excluding erythrocytes and debris. Set the threshold on DCV-H to eliminate electronically DCV-negative events (Figure 1A).

   As DCV is a cell permeable DNA stain, negative DCV events correspond to non-nucleated cells (platelets, erythrocytes) and debris. A DCV threshold reduces the number of events electronically captured and consequently allowing a better acquisition display.

6. Create a dual density/dot plot displaying SSC-H on a linear scale vs 7-AAD-H on a logarithmic scale to exclude necrotic cells.
7. Create a dual density/dot plot displaying DCV-H vs DCV-A on a logarithmic scale for doublets and aggregates discrimination.
8. Create a dual density/dot plot displaying FSC-H vs SSC-H, both on a linear scale to visualize the leukocytes.
9. Create a dual density/dot plot displaying SSC-H vs each fluorochrome to adjust the autofluorescence (Figure 1B).
10. Create dual density/dot plot displaying all fluorochrome combinations on a logarithmic scale for color compensation verification (Figure 1C). The labeling panel is shown in Table 1.

Sample acquisition

11. Run the sample and adjust SSC and DCV parameters with the SSC-H vs DCV-H density/dot plot. Set the threshold empirically on DCV-H to capture nucleated cells and exclude erythrocytes and debris.

12. Adjust FSC-H on a FSC-H vs SSC-H density/dot plot.
13. Adjust voltages for the 7-AAD signal on a SSC-H vs 7-AAD-H density/dot plot. Adjust CD33-PE-Cy7, CD11b-APC, HLA-DR-FITC and PD-L1-PE voltages in the same way.

    When performing the protocol, prepare a negative control to detect autofluorescence and a Fluorescent Minus One (FMO) control for each of the four markers. Compensate overlapping fluorochrome spectra. Spillover values calculated for this protocol are shown in supplementary table 1.

14. Acquire the sample at a flow rate of 25 µl/min and collect at least 50,000 DCV-positive gated cells using the gating strategy detailed below.

For each prepared sample, first analyze the tube prepared with DMSO (negative control) and then the stimulated cells with PMA. If more than one sample is prepared, rinse or run blank sample to avoid sample contamination.

Gating strategy

15. On a SSC-H vs DCV-H dual plot, draw a region for DCV-positive events (R1; nucleated cells), and set the R1 gate on a SSC-H vs 7-AAD-H dual plot (Figure 2).
16. Draw a second region for 7-ADD- cells (R2; non-necrotic cells) on a SSC-H vs 7-AAD-H dual plot, and set a the R2 gate on a DCV-H versus DCV-A dual plot.
17. Draw a third region (R3) for single cells on a DCV-H versus DCV-A dual plot and set the R3 gate on a FSC-H versus SSC-H dual plot.
18. Draw a fourth region (R4) on a FSC-H versus SSC-H dual plot for leukocytes and set the R4 gate on a CD33-H versus CD11b-H dual plot.
19. Draw a fifth region (R5) on a CD33-H versus CD11b-H dual plot for $CD33^{+}CD11b^{+}$ cells selection and set a gate (R5) on a FSC-H versus HLA-DR-H dual plot.
20. Draw a sixth region (R6) on a FSC-H versus HLA-DR-H dual plot for MDSCs selection and set the R6 gate on a FSC-H versus PD-L1-H dual plot.
21. Draw a seventh region (R7) on a FSC-H versus PD-L1-H dual plot for $PD\text{-}L1^{+}$ MDSCs selection and set the R7 gate on a CD33-H versus CD11b-H dual plot.
22. On the CD33-H versus CD11b-H dual plot displaying events in R7, delimitate the M-MDSCs with a region (R8) based on the $CD33^{hi}CD11b^{+}$ expression pattern. Draw another region (R9) for the $CD11b^{hi}CD33^{+}$ PMN-MDSCs.

SUPPORT PROTOCOL 1:

Bioinformatic tools for the analysis of flow cytometric data

Flow cytometric data obtained can be further condensed and reduced into two dimensions, enabling a simplified display of high-dimensional and complex results. There are several bioinformatic approaches that can be performed on this data: t-SNE (T-distributed Stochastic Neighbor Embedding), UMAP (Uniform Manifold Approximation and Projection), and FlowSOM (Flow Self-Organizing Map). t-SNE and UMAP are based on a random algorithm that reduces all the variables into a 2-dimension plot (Becht et al., 2019; Mcinnes et al., 2020; Van Der Maaten & Hinton, 2008). The FlowSOM algorithm groups together cells that share expression of the selected variables, therefore defining and sorting populations (Van Gassen et al., 2015). The data must be processed into a unique concatenated file where subgroups can be defined by selection. These three approaches are all performed by selecting the variables corresponding to the height pulse of the MDSC lineage markers. This support protocol describes how to analyze flow cytometry data by using these tools.

Materials:

Flow Cytometry Standard (FCS) files obtained from sample acquisition (see Basic Protocol 2).
FlowJo™ v10.8 analysis software.
FlowJo Plugins

- tSNE plugin (included in FlowJo analysis software)
- UMAP plugin version 4.0.4 (downloaded from FlowJo Exchange plugins)
- FlowSOM plugin version 3.0.18 (downloaded from FlowJo Exchange plugins)

Protocol steps with step annotations:

1. Analyze the FCS files in the analysis software with the gating strategy mentioned in Basic Protocol 1.
2. Classify the samples according to stimulation condition and sample label number.

   Following these recommendations, it will be possible to select DMSO and PMA as a group. Classification can easily be done by adding the keyword "stimulation" to each FCS file.

3. Identify and select the myeloid-derived suppressor cell population from all samples and concatenate them.

   If the bioinformatic tool selected does not support a large number of events, reduce the number of cells considered from each sample in the process of concatenating. Otherwise, if downsampling is performed over the concatenated file, the event reduction will not be performed equitably in all samples.

4. Plot SampleID from the concatenated file to display the samples included and identify the different groups (in this case, "stimulation" group)
5. Run tSNE and UMAP on the concatenated file selecting the lineage marker channels corresponding to the height pulse (PD-L1-H, HLA-DR-H, CD33-H and CD11b-H) (Figure 3). Perform these approaches in the whole file in order to include all the information. Afterwards, a single subgroup can be selected and isolated for visualization.
6. Run FlowSOM on the concatenated file selecting the lineage marker channels corresponding to the height pulse (PD-L1-H, HLA-DR-H, CD33-H and CD11b-H) (Figure 4).

   Selecting "scale" is recommended to normalize and better visualize the expression of lineage markers.

7. Run other FlowSOMs for unstimulated and stimulated conditions by selecting the previously generated FlowSOM in the "apply on map" option.

   As FlowSOM is based in random distribution, if analyzing further subgroups, it is best to select the "apply on map" feature to preserve the structure and distribution of all the data and eventually obtain comparable maps.

8. Backgate the populations listed in the background legend (metaclusters) to characterize each population's phenotype.

REAGENTS AND SOLUTIONS:

HBA

- Hanks' balanced salt solution, calcium- and magnesium-free, without phenol red (Capricorn Scientific GmbH, cat. no. HBSS-2A).
- 1% Bovine Serum Albumin (Sigma-Aldrich®, cat. no. A7906)
- 0.1% NaN_3; Sodium Azide extra pure (Sigma-Aldrich®, cat. no. 71290)

  Store up to 6 months at 4 °C.

PMA 1 mg/ml

- Phorbol 12-myristate 13-acetate (PMA) (Sigma-Aldrich®, cat. no. P8139-1MG)
- Anhydrous dimethyl sulfoxide (DMSO, Invitrogen™, cat. no. D12345)
  Add 1 ml DMSO to one vial containing 1 mg PMA to prepare 1 mg/ml solution.

  Once prepared, the solution should be stored up to 6 months at 4 °C. For longer storage, maintain stock solutions at -20 °C.

Türk solution

- 0.01% (v/v) Giemsa stain
- 3% (v/v) acetic acid
- 10 mM HEPES 99.9% purity (Merk, cat. no. H3375-25G)

Store up to a month at room temperature.

7-AAD 1 mg/ml

- 7-Aminoactinomycin D (7-AAD, Invitrogen™, cat. no. A1310)
- Anhydrous dimethyl sulfoxide (DMSO, Invitrogen™, cat. no. D12345)
  Add 1 ml DMSO to one vial containing 1 mg 7-AAD to prepare 1 mg/ml solution.

Once prepared, the solution can be stored up to 6 months at 4 °C.

COMMENTARY:

Background Information:

Immunotherapy has been gaining relevance among cancer therapy strategies over the last years and its action is proving beneficial for the treatment of many other diseases. In the case of solid tumors, such as non-small-cell lung cancer (NSCLC), cancer immunotherapy has become a promising strategy since modulating the immune system leads toward a long-term survival outcome, with a more targeted strategy and a lower toxicity profile (Mamdani et al., 2022; Passiglia et al., 2016). The most commonly targeted immune checkpoint is the Programmed Cell Death Protein 1/Programmed Cell Death Protein Ligand 1 (PD-1/PD-L1), which constitutes a prominent and valuable target. The PD-1 receptor is mainly expressed in activated T lymphocytes while its ligand, PD-L1, is expressed in antigen-presenting cells, Myeloid-Derived Suppressor Cells (MDSCs), some non-hematopoietic cells, and tumoral cells. This inhibitory checkpoint naturally prevents exacerbated autoimmune responses by inducing T cell downregulation and apoptosis. Interestingly, it is also used by the tumor microenvironment as a tumor immune escape mechanism (Freeman et al., 2000; Yamazaki et al., 2002; Youn et al., 2008). Concerning NSCLC, tumoral PD-L1 expression is a determinant for immunotherapy election, allowing the identification of those patients who are supposed to benefit from the anti-PD-1/PD-L1 therapy and their classification into the different treatment lines (Lantuéjoul et al., 2020).

Qualitative immunohistochemical assays using monoclonal mouse anti-PD-L1 are currently approved commercial assays available to assess PD-L1 levels in cancer patients. PD-L1 protein expression in NSCLC is determined by using Tumor Proportion Score (TPS), which is the percentage of viable tumor cells that exhibit partial or complete membrane staining at any intensity (Ettinger et al., 2021). There are currently four approved commercial assays available to assess PD-L1 levels in NSCLC patients (Paver et al., 2021). Each assay is drug-specific and has a specific threshold for positivity: (1) The Ventana SP142 Assay, which is intended for atezolizumab treatment; (2) the Ventana SP263 assay, which is intended for patients treated with pembrolizumab or durvalumab; (3) the Dako 22C3 assay, for pembrolizumab only; and (4) the Dako 28-8 assay, for nivolumab-treated patients. PD-L1 determination can also be performed using primary antibodies such as E1L3N or QR1, as a complementary procedure to diagnosis. Several studies reveal high concordance using SP263, 22C3 and 28-8 when assessing PD-L1 expression in tumor cells (Adam et al., 2018; Hirsch et al., 2017; Ratcliffe et al., 2017; Scheel et al., 2016; Skov & Skov, 2017), whereas SP142 assay reveals PD-L1 lower expression (Adam et al., 2018; Hirsch et al., 2017; Ilie et al., 2016; Rimm et al., 2017; Scheel et al., 2016). Comparisons with noncommercial IHC assays reveal high variability in the concordance of the PD-L1 expression results, that can lead to misclassifications (Adam et al., 2018; Cogswell et al., 2017; Scheel et al., 2018; Smith et al., 2016). Moreover, the study of PD-L1 by immunohistochemistry (IHC) in immune cells is limited to tumor-infiltrating cells, and it also exhibits high variability for the assessment of PD-L1 levels (Rehman et al., 2017; Rimm et al., 2017). This discordance could be explained by uncontrolled pre-analytical variables, or sample bias due to PD-L1 expression heterogeneity (Kolb et al., 2023). Additionally, to avoid misclassifications, PD-L1 assessment by IHC requires specific training or specialized pathologists to maintain consistency and quality of interpretation, as well as a laboratory validation of the assay and continuous quality monitoring (Fernandez et al., 2023).

The existing differences in PD-L1 IHC assays raise questions about their comparability and diagnostic use and their difficult harmonization, reproducibility and standardization. Generally, a higher PD-L1 expression correlates with a better immunotherapy response (Woodford et al., 2022), although this association remains unclear. A nivolumab study shows that the efficacy of the drug was independent of the PD-L1 expression (Brahmer et al., 2015) and another study states that NSCLC

patients with PD-L1-negative tumors have a better outcome with pembrolizumab plus chemotherapy in comparison with chemotherapy alone (Borghaei et al., 2020). Other studies state that patients with PD-L1 positive tumors (TPS ≥ 50%) had significant higher responses to immunotherapy drugs compared to PD-L1 negative tumors (Passiglia et al., 2016; Reck et al., 2016). Some authors propose that this inconsistency may be explained by the lack of unique guidelines and a reference model to assess PD-L1 expression. Firstly, different cut-off values are set to consider PD-L1 positivity among studies (TPS ≥ 1 to 50%). Secondly, regarding technical questions, four PD-L1 immunohistochemistry assays are registered with the FDA, employing four different antibodies and two immunohistochemistry platforms with their own scoring systems. Thirdly, the heterogeneity of PD-L1 expression in the tissue along with the tiny size of biopsies lead to PD-L1 under- or overestimation (Kolb et al., 2023). All those variables contribute to a different outcome for PD-L1 expression among studies (Ancevski Hunter et al., 2018; Xu et al., 2017). Finally, the dynamic changes in PD-L1 expression may also contribute to impair the quality of the results obtained (Yue et al., 2018).

Although anti-PD-1/PD-L1 immunotherapy has clearly improved the clinical outcome in solid tumors, the overall survival is still low. Currently, mostly 15 to 25% of patients with advanced NSCLC that undergo immunotherapy demonstrate an objective response rate from this therapeutic approach (Akinboro et al., 2022; Brahmer et al., 2015; Garon et al., 2015; Gettinger et al., 2019; Paz-Ares et al., 2022). Indeed, a better understanding and characterization of this immune checkpoint inhibitor and the immune system is mandatory. In this work, the authors have described a flow cytometric protocol to assess the PD-L1 levels in Myeloid-Derived Suppressor Cells. PD-L1 is detected with a stimulatory assay by means of a minimal sample perturbation protocol, aimed at the preservation of the sample in its native state. Using this minimally invasive approach, this protocol is a good alternative for PD-L1 screening in peripheral blood. In fact, this protocol may be complementary used for the assessment of PD-L1 TPS for diagnostic purposes in cancer.

Critical Parameters:

Peripheral blood samples should be processed immediately after drawing, ideally within the first 4 hours. If the samples cannot be analyzed immediately, then they should be stored at room temperature, preferably in gentle agitation to preserve sample integrity as much as possible.

Unlysed whole-blood samples contain a large ratio of erythrocytes relative to leukocytes (700:1 approximately) that greatly impacts light scatter data, and these erythrocytes must be omitted from the acquisition. Setting a fluorescent threshold and using DNA viable stains (i.e., DCV, Hoechst 33342, SYTO13, and others), it is possible to electronically discard non-nucleated events (erythrocytes and platelets) and debris on the flow cytometer. Importantly, when performing experiments involving unlysed whole blood, the height parameter (H) should be used, providing scatter and fluorescent signals for the different leukocyte populations. When using area (A), erythrocytes contribute more to the light scatter, which results in high coincidence with leukocytes. Using the violet side scatter will result in even better resolution of the target populations.

For an accurate leukocyte scatter, the event rate should be established depending on the flow cytometer used. For best-quality data, plan for event rates below the Poisson 10% coincident rate of an instrument, at which 90% of cells can be classified as singlets.

PD-L1 detection can be negatively influenced by some factors. Firstly, different anti-PD-L1 antibody clones can result in differential reactivity based on different epitope specificity and affinity. Secondly, sample manipulation may also affect the reactivity and the identification of the target cells. The use of some fixative agents, such as paraformaldehyde, can result in differential reactivity against the antibody used. Moreover, when culturing adherent cells, cell detachment using enzymatic digestion may also have an important effect in the identification of target cells, and enzyme-free alternative methods are recommended.

Troubleshooting:

Tables 2, 3 and 4 list problems that may arise when following this protocol as well as their causes and potential solutions.

Understanding Results:

PD-L1 molecule can be detected by flow cytometry in circulating myeloid-derived suppressor cells following Basic Protocol 1. This protocol uses minimal perturbation of the peripheral whole blood sample, avoiding any lysis or washing steps and preserving cell function and structure (Petriz et al., 2018; Rico, Salvia, et al., 2021).

PD-L1 detection is an important step for diagnosis and treatment eligibility in many oncologic diseases. For example, in non-small-cell lung cancer, pembrolizumab monotherapy requires ≥50% PD-L1-stained tumor cells in first-line treatment and ≥1% in second-line treatment (Reck et al., 2016). Currently, a small number of NSCLC patients meet the criteria to undergo anti-PD-1/PD-L1 immunotherapy, and it is crucial to identify all potential patients who would benefit from these immune checkpoint inhibitors (Califano et al., 2018). In the clinic, the only approved methodology to quantify this biomarker is immunohistochemistry (IHC) of fixed biopsies, which reports PD-L1 levels in the tumor. The main problem consists in the variability of PD-L1 IHC results, as there are four different IHC assays which may have different thresholds and scoring scheme (Ancevski Hunter et al., 2018; Xu et al., 2017).

Interestingly, Basic Protocol 1 and 2 defines a complementary and non-invasive analysis that helps to capture the overall status of the patient's immune system by analyzing PD-L1 expression in circulating MDSCs. In fact, it has been described that MDSCs correlate with a worse outcome in NSCLC (Barrera et al., 2018; Bronte et al., 2022; Yamauchi et al., 2018). Therefore, detection of circulating PD-L1+ MDSCs may stand as a putative and complementary biomarker test.

After following all steps of Basic Protocol 2, the authors obtained a complete panel (Figure 1) used to discriminate the leukocyte compartment from background and necrotic cells, and to finally identify MDSCs based on $CD11b^{+}CD33^{+}HLA\text{-}DR^{low/-}$ staining. In addition, this panel allows the characterization of the two subtypes of MDSCs based on their differential expression of myeloid surface markers, being $CD11b^{+}/CD33^{hi}$ MDSCs monocytic and $CD11b^{hi}/CD33^{+}$ MDSCs polymorphonuclear, without the need to add further fluorophores such as CD14 or CD15. In order to obtain accurate results, samples should be prepared as specified in Basic Protocol Protocol 1, using a minimal sample perturbation method in combination with a stimulatory assay.

Importantly, the PD-L1 ligand remains elusive to the targeting of the α-PD-L1 antibody in MDSCs. In this case, phorbol ester (PMA) stimulation is successfully used to unmask the ligand. Therefore, in the absence of stimulation, PD-L1 is not detected in peripheral blood MDSCs obtained from NSCLC patients (Figure 2A). However, PD-L1 reactivity dramatically increases after PMA stimulation (Figure 2B), making the identification of the PD-L1+ MDSC population feasible (Rico, Aguilar Hernández, et al., 2021). One of the artifacts that can occur when performing the protocol is that stimulation with PMA can result in an increased autofluorescence, and further gating readjustment may be needed. The authors have analyzed peripheral blood specimens obtained from NSCLC patients after PMA stimulation and without any stimulation (DMSO) and hypothesize that upon stimulation with PMA, PD-L1 molecule suffers conformational changes that allow the targeting of the epitopic site. The authors have performed additional experiments involving intracellular staining of PD-L1 in order to rule out the possibility of PD-L1 translocation from the cytoplasm to the cell membrane (data not shown).

The mechanism of action and immunosuppressive activity of MDSCs are influenced by their subtype and localization. MDSCs present soluble antigens through MHC class I and induce T cells unresponsiveness by reactive oxygen species (ROS) in an antigen-dependent manner. On the flip side, in the tumor microenvironment (TME), MDSCs become more suppressive and mediate antigen-nonspecific immunosuppression of T cells by nitric oxide (NO) production and arginase activity. In secondary lymphoid organs the main subset are PMN-MDSCs, which participate in tumor-specific T cell tolerance. In the TME, M-MDSCs are more prominent than PMN-MDSCs and rapidly differentiate into tumor-associated macrophages (Corzo et al., 2010; Gabrilovich & Nagaraj, 2009; Kumar et al., 2016; Movahedi et al., 2008). In NSCLC patients, it has been reported that the highest levels of M-MDSC are found in peripheral blood, in relation to tumor tissue or lymph nodes (Pogoda et al., 2016), even though the main population in peripheral blood corresponds to PMN-MDSCs (Kumar et al., 2016). The circulating M-MDSC subset is significantly increased compared to healthy donors (Heuvers et al., 2013; Huang et al., 2013; Yamauchi et al., 2018) and is associated with poor overall survival (Bronte et al., 2022; Zahran et al., 2021). Regarding polymorphonuclear MDSCs, there is a higher percentage in peripheral blood of NSCLC patients compared to healthy donors, along with higher levels of arginase 1 (Barrera et al., 2018; Heuvers et al., 2013; Tian et al., 2021).

Bioinformatics algorithms have emerged as remarkable tools for comprehensive analysis and representation of flow cytometry data, enabling simplified visualization of complex, high-dimensional results. The tSNE and UMAP algorithms reduce data to two-dimensional space and cluster events based on similarity to reveal local data structure and identify distinct cell populations (Becht et al., 2019; Mcinnes et al., 2020; Van Der Maaten & Hinton, 2008).

Figure 3 shows an example for selecting the H-pulse on the lineage markers. In addition, FlowSOM allows us to find cell subsets and classifications that may not be apparent at first glance (Van Gassen et al., 2015) (Figure 4). In fact, these approaches allow different visualizations of the data and to quickly see changes in populations or in their particular expression. For example, tSNE and UMAP can graphically describe populations based on particular markers, while FlowSOM can develop a specific profile for each condition/group and predict an individual classification.

This protocol allows a rapid and non-invasive assessment of PD-L1-expressing MDSCs from peripheral blood in cancer patients. The methodology preserves the native function of the PD-L1 molecule and allows its accurate identification in MDSCs, with PD-

L1 being a potential biomarker to help predict response to treatment. Since MDSCs are associated with worse survival, the accurate identification and targeting of these cells is critical to assess the patient's status in relation to their cancer. Thus, this flow cytometry protocol may serve as a complementary test to IHC assays to report PD-L1 expression and the immune status of the patient.

Time Considerations:

The time needed to perform each of the protocol steps should be as follows:

- Basic Protocol 1:
- Sample preparation: 45 minBasic Protocol 2:
  - Flow cytometer setup: 15 min
  - Protocol preparation: 10 min
  - Sample acquisition: 5 min
  - Gating strategy: 10 min
- Support Protocol 1:
  - Bioinformatic analysis: 1-2 hours

CONFLICT OF INTEREST STATEMENT:

M.D.W. and J.A.B. work for Thermo Fisher Scientific, which is in the business of selling flow cytometers and flow cytometry reagents.

DATA AVAILABILITY STATEMENT:

The data that support the protocol is available from the corresponding author upon reasonable request.

ACKNOWLEDGEMENTS:

This study was partially supported by Thermo Fisher Scientific. We thank the CERCA Programme/Generalitat de Catalunya, and the Germans Trias i Pujol Foundation for institutional support, and also acknowledge financial support from the Obra Social la Caixa. The authors are very grateful to Dr. Teresa Morán and the Immunology Laboratory of the Hospital Germans Trias i Pujol for coordinating and providing the samples, and to Clara Streiff, Paola Paglia, Sergio Ramon, Lluís Sainz, and Víctor Querol from Thermo Fisher Scientific for all their help in this research field. Part of this work was done while the corresponding author was principal investigator at the Josep Carreras Leukaemia Research Institute (Spain).

LITERATURE CITED:

Adam, J., Le Stang, N., Rouquette, I., Cazes, A., Badoual, C., Pinot-Roussel, H., Tixier, L., Danel, C., Damiola, F., Damotte, D., Penault-Llorca, F., & Lantuéjoul, S. (2018). Multicenter harmonization study for PD-L1 IHC testing in non-small-cell lung cancer. *Annals of Oncology*, *29*(4), 953–958. https://doi.org/10.1093/annonc/mdy014

Ahmed, M., & Barakat, K. (2017). The Too Many Faces of PD-L1: A Comprehensive Conformational Analysis Study. *Biochemistry*, *56*(40), 5428–5439. https://doi.org/10.1021/acs.biochem.7b00655

Akinboro, O., Larkins, E., Pai-Scherf, L. H., Mathieu, L. N., Ren, Y., Cheng, J., Fiero, M. H., Fu, W., Bi, Y., Kalavar, S., Jafri, S., Mishra-Kalyani, P. S., Zirkelbach, J. F., Li, H., Zhao, H., He, K., Helms, W. S., Chuk, M. K., Wang, M., … Singh, H. (2022). FDA Approval Summary: Pembrolizumab, Atezolizumab, and Cemiplimab-rwlc as Single Agents for First-Line Treatment of Advanced/Metastatic PD-L1–High NSCLC. *Clinical Cancer Research*, *28*(11), 2221–2228. https://doi.org/10.1158/1078-0432.CCR-21-3844

Ancevski Hunter, K., Socinski, M. A., & Villaruz, L. C. (2018). PD-L1 Testing in Guiding Patient Selection for PD-1/PD-L1 Inhibitor Therapy in Lung Cancer. *Molecular Diagnosis and Therapy*, *22*(1), 1–10. https://doi.org/10.1007/s40291-017-0308-6

Barrera, L., Montes-Servín, E., Hernandez-Martinez, J. M., Orozco-Morales, M., Montes-Servín, E., Michel-Tello, D., Morales-Flores, R. A., Flores-Estrada, D., & Arrieta, O. (2018). Levels of peripheral blood polymorphonuclear myeloid-derived suppressor cells and selected cytokines are potentially prognostic of disease progression for patients with non-small cell lung cancer. *Cancer Immunology, Immunotherapy*, *67*(9), 1393–1406. https://doi.org/10.1007/s00262-018-2196-y

Becht, E., McInnes, L., Healy, J., Dutertre, C. A., Kwok, I. W. H., Ng, L. G., Ginhoux, F., & Newell, E. W. (2019). Dimensionality reduction for visualizing single-cell data using UMAP. *Nature Biotechnology*, *37*(1), 38–47. https://doi.org/10.1038/nbt.4314

Borghaei, H., Langer, C. J., Paz-Ares, L., Rodríguez-Abreu, D., Halmos, B., Garassino, M. C., Houghton, B., Kurata, T., Cheng, Y., Lin, J., Pietanza, M. C., Piperdi, B., & Gadgeel, S. M. (2020). Pembrolizumab plus chemotherapy versus chemotherapy alone in patients with advanced non–small cell lung cancer without tumor PD-L1 expression: A pooled analysis of 3 randomized controlled trials. *Cancer*, *126*(22), 4867–4877. https://doi.org/10.1002/cncr.33142

Brahmer, J., Reckamp, K. L., Baas, P., Crinò, L., Eberhardt, W. E. E., Poddubskaya, E., Antonia, S., Pluzanski, A., Vokes, E. E., Holgado, E., Waterhouse, D., Ready, N., Gainor, J., Arén Frontera, O., Havel, L., Steins, M., Garassino, M. C., Aerts, J. G., Domine, M., … Spigel, D. R. (2015). Nivolumab versus Docetaxel in Advanced Squamous-Cell Non–Small-Cell Lung Cancer. *New England Journal of Medicine*, *373*(2), 123–135. https://doi.org/10.1056/nejmoa1504627

Bronte, G., Petracci, E., De Matteis, S., Canale, M., Zampiva, I., Priano, I., Cravero, P., Andrikou, K., Burgio, M. A., Ulivi, P., Delmonte, A., & Crinò, L. (2022). High Levels of Circulating Monocytic Myeloid-Derived Suppressive-Like Cells Are Associated With the Primary Resistance to Immune Checkpoint Inhibitors in Advanced Non-Small Cell Lung Cancer: An Exploratory Analysis. *Frontiers in Immunology*, *13*(April), 1–10. https://doi.org/10.3389/fimmu.2022.866561

Califano, R., Lal, R., Lewanski, C., Nicolson, M. C., Ottensmeier, C. H., Popat, S., Hodgson, M., & Postmus, P. E. (2018). Patient selection for anti-PD-1/PD-L1 therapy in advanced non-small-cell lung cancer: Implications for clinical practice. *Future Oncology*, *14*(23), 2415–2431. https://doi.org/10.2217/fon-2018-0330

Campos-Escamilla, C., Siliqi, D., Gonzalez-Ramirez, L. A., Lopez-Sanchez, C., Gavira, J. A., & Moreno, A. (2021). X-ray characterization of conformational changes of human apo- and holo-transferrin. *International Journal of Molecular Sciences*, *22*(24). https://doi.org/10.3390/ijms222413392

Cogswell, J., Inzunza, H. D., Wu, Q., Feder, J. N., Mintier, G., Novotny, J., & Cardona, D. M. (2017). An Analytical Comparison of Dako 28-8 PharmDx Assay and an E1L3N Laboratory-Developed Test in the Immunohistochemical Detection of Programmed Death-Ligand 1. *Molecular Diagnosis and Therapy*, *21*(1), 85–93. https://doi.org/10.1007/s40291-016-0237-9

Corzo, C. A., Condamine, T., Lu, L., Cotter, M. J., Youn, J. I., Cheng, P., Cho, H. Il, Celis, E., Quiceno, D. G., Padhya, T., McCaffrey, T. V., McCaffrey, J. C., & Gabrilovich, D. I. (2010). HIF-1α regulates function and differentiation of myeloid-derived suppressor cells in the tumor microenvironment. *Journal of Experimental Medicine*, *207*(11), 2439–2453. https://doi.org/10.1084/jem.20100587

Ding, K., Yi, M., Liang, H., Li, Z., & Zhang, Y. (2022). Efficacy comparison of immune treating strategies for NSCLC patients with negative PD-L1 expression. *Expert Review of Clinical Immunology*, *18*(7), 759–771. https://doi.org/10.1080/1744666X.2022.2088510

Ettinger, D. S., Wood, D. E., Aisner, D. L., Akerley, W., Bauman, J. R., Bharat, A., Bruno, D. S., Chang, J. Y., Chirieac, L. R., D'Amico, T. A., Dilling, T. J., Dowell, J., Gettinger, S., Gubens, M. A., Hegde, A., Hennon, M., Lackner, R. P., Lanuti, M., Leal, T. A., … Hughes, M. (2021). Non-Small Cell Lung Cancer, Version 2.2021 Featured Updates to the NCCN Guidelines. *JNCCN Journal of the National Comprehensive Cancer Network*, *19*(3), 254–266. https://doi.org/10.6004/jnccn.2021.0013

Feng, M., Gao, W., Wang, R., Chen, W., Man, Y. G., Figg, W. D., Wang, X. W., Dimitrov, D. S., & Ho, M. (2013). Therapeutically targeting glypican-3 via a conformation-specific single-domain antibody in hepatocellular carcinoma. *Proceedings of the National Academy of Sciences of the United States of America*, *110*(12). https://doi.org/10.1073/pnas.1217868110

Fernandez, A. I., Robbins, C. J., Gaule, P., Agostini-vulaj, D., Anders, R. A., Bellizi, A., Chen, W., Eric, Z., Gopal, P., Zhao, L., Lisovsky, M., Liu, X., Shia, J., Wang, H., Yang, Z., Mccann, L., Chan, Y. G., Weidler, J., Bates, M., … Rimm, D. L. (2023). Multi-Institutional Study of Pathologist Reading of the Programmed Cell Death Ligand-1 Combined Positive Score Immunohistochemistry Assay for Gastric or Gastroesophageal Junction Cancer. *Modern Pathology*, *36*(5), 100128. https://doi.org/https://doi.org/10.1016/j.modpat.2023.100128

Freeman, B. G. J., Long, A. J., Iwai, Y., Bourque, K., Chernova, T., Nishimura, H., Fitz, L. J., Malenkovich, N., Okazaki, T., Byrne, M. C., Horton, H. F., Fouser, L., Carter, L., Ling, V., Bowman, M. R., Carreno, B. M., Collins, M., Wood, C. R., & Honjo, T. (2000). Engagement of the PD-1 Immunoinhibitory Receptor by a Novel B7 Family Member Leads to Negative Regulation of Lymphocyte Activation. *Journal of Experimental Medicine*, *192*(7), 1028–1034.

Gabrilovich, D. I., & Nagaraj, S. (2009). Myeloid-derived suppressor cells as regulators of the immune system. *Nature c*, *9*(3), 162–174. https://doi.org/10.1038/nri2506

Garon, E. B., Rizvi, N. A., Hui, R., Leighl, N., Balmanoukian, A. S., Eder, J. P., Patnaik, A., Aggarwal, C., Gubens, M., Horn, L., Carcereny, E., Ahn, M.-J., Felip, E., Lee, J.-S., Hellmann, M. D., Hamid, O., Goldman, J. W., Soria, J.-C., Dolled-Filhart, M., … Gandhi, L. (2015). Pembrolizumab for the Treatment of Non–Small-Cell Lung Cancer. *New England Journal of Medicine*, *372*(21), 2018–2028. https://doi.org/10.1056/nejmoa1501824

Gettinger, S., Borghaei, H., Brahmer, J., Chow, L., Burgio, M., De Castro Carpeno, J., Pluzanski, A., Arrieta, O., Frontera, O. A., Chiari, R., Butts, C., Wojcik-Tomaszewska, J., Coudert, B., Garassino, M., Ready, N., Felip, E., Garcia, M. A., Waterhouse, D., Domine, M., … Vokes, E. (2019). OA14.04 Five-Year Outcomes From the Randomized, Phase 3 Trials CheckMate 017/057: Nivolumab vs Docetaxel in Previously Treated NSCLC. *Journal of Thoracic Oncology*, *14*(10), S244–S245. https://doi.org/10.1016/j.jtho.2019.08.486

Henderson, J., Havranek, O., Ma, M. C. J., Herman, V., Kupcova, K., Chrbolkova, T., Pacheco-Blanco, M., Wang, Z., Comer, J. M., Zal, T., & Davis, R. E. (2022). Detecting Förster resonance energy transfer in living cells by conventional and spectral flow cytometry. *Cytometry Part A*, *101*(10), 818–834. https://doi.org/10.1002/cyto.a.24472

Heuvers, M. E., Muskens, F., Bezemer, K., Lambers, M., Dingemans, A. M. C., Groen, H. J. M., Smit, E. F., Hoogsteden, H. C., Hegmans, J. P. J. J., & Aerts, J. G. J. V. (2013). Arginase-1 mRNA expression correlates with myeloid-derived suppressor cell levels in peripheral blood of NSCLC patients. *Lung Cancer*, *81*(3), 468–474. https://doi.org/10.1016/j.lungcan.2013.06.005

Hirsch, F. R., McElhinny, A., Stanforth, D., Ranger-Moore, J., Jansson, M., Kulangara, K., Richardson, W., Towne, P., Hanks, D., Vennapusa, B., Mistry, A., Kalamegham, R., Averbuch, S., Novotny, J., Rubin, E., Emancipator, K., McCaffery, I., Williams, J. A., Walker, J., … Kerr, K. M. (2017). PD-L1 Immunohistochemistry Assays for Lung Cancer: Results from Phase 1 of the Blueprint PD-L1 IHC Assay Comparison Project. *Journal of Thoracic Oncology*, *12*(2), 208–222. https://doi.org/10.1016/j.jtho.2016.11.2228

Hoechst, B., Ormandy, L. A., Ballmaier, M., Lehner, F., Krüger, C., Manns, M. P., Greten, T. F., & Korangy, F. (2008). A New Population of Myeloid-Derived Suppressor Cells in Hepatocellular Carcinoma Patients Induces CD4+CD25+Foxp3+ T Cells. *Gastroenterology*, *135*(1), 234–243. https://doi.org/10.1053/j.gastro.2008.03.020

Huang, A., Zhang, B., Wang, B., Zhang, F., Fan, K. X., & Guo, Y. J. (2013). Increased CD14+HLA-DR-/low myeloid-derived suppressor cells correlate with extrathoracic metastasis and poor response to chemotherapy in non-small cell lung cancer patients. *Cancer Immunology, Immunotherapy*, *62*(9), 1439–1451. https://doi.org/10.1007/s00262-013-1450-6

Ilie, M., Long-Mira, E., Bence, C., Butori, C., Lassalle, S., Bouhlel, L., Fazzalari, L., Zahaf, K., Lalvée, S., Washetine, K., Mouroux, J., Vénissac, N., Poudenx, M., Otto, J., Sabourin, J. C., Marquette, C. H., Hofman, V., & Hofman, P. (2016). Comparative study of the PD-L1 status between surgically resected specimens and matched biopsies of NSCLC patients reveal major discordances: A potential issue for anti-PD-L1 therapeutic strategies. *Annals of Oncology*, *27*(1), 147–153. https://doi.org/10.1093/annonc/mdv489

Koh, J., Kim, Y., Lee, K. Y., Hur, J. Y., Kim, M. S., Kim, B., Cho, H. J., Lee, Y. C., Bae, Y. H., Ku, B. M., Sun, J.-M. M., Lee, S.-H. H., Ahn, J. S., Park, K., & Ahn, M.-J. J. (2020). MDSC subtypes and CD39 expression on CD8+ T cells predict the efficacy of anti-PD-1 immunotherapy in patients with advanced NSCLC. *European Journal of Immunology*, *50*(11), 1810–1819. https://doi.org/10.1002/eji.202048534

Kolb, T., Benckendorff, J., Möller, P., Barth, T. F. E., & Marienfeld, R. B. (2023). Heterogeneous expression of predictive biomarkers PD-L1 and TIGIT in non-mucinous lung adenocarcinoma and corresponding lymph node metastasis: A challenge for clinical biomarker testing. *Neoplasia (United States)*, *38*(October 2022), 100884. https://doi.org/10.1016/j.neo.2023.100884

Kumar, V., Patel, S., Tcyganov, E., & Gabrilovich, D. I. (2016). The Nature of Myeloid-Derived Suppressor Cells in the Tumor Microenvironment. *Trends in Immunology*, *37*(3), 208–220. https://doi.org/10.1016/j.it.2016.01.004

Lantuéjoul, S., Sound-Tsao, M., Cooper, W. A., Girard, N., Hirsch, F. R., Roden, A. C., Lopez-Rios, F., Jain, D., Chou, T. Y., Motoi, N., Kerr, K. M., Yatabe, Y., Brambilla, E., Longshore, J., Papotti, M., Sholl, L. M., Thunnissen, E., Rekhtman, N., Borczuk, A., … Mino-Kenudson, M. (2020). PD-L1 Testing for Lung Cancer in 2019: Perspective From the IASLC Pathology Committee. *Journal of Thoracic Oncology*, *15*(4), 499–519. https://doi.org/10.1016/j.jtho.2019.12.107

Latorraca, N. R., Venkatakrishnan, A. J., & Dror, R. O. (2017). GPCR dynamics: Structures in motion. In *Chemical Reviews* (Vol. 117, Issue 1, pp. 139–155). American Chemical Society. https://doi.org/10.1021/acs.chemrev.6b00177

Lin, D. Y. W., Tanaka, Y., Iwasaki, M., Gittis, A. G., Su, H. P., Mikami, B., Okazaki, T., Honjo, T., Minato, N., & Garboczi, D. N. (2008). The PD-1/PD-L1 complex resembles the antigen-binding Fv domains of antibodies and T cell receptors. *Proceedings of the National Academy of Sciences of the United States of America*, *105*(8), 3011–3016. https://doi.org/10.1073/pnas.0712278105

Mamdani, H., Matosevic, S., Khalid, A. B., Durm, G., & Jalal, S. I. (2022). Immunotherapy in Lung Cancer: Current Landscape and Future Directions. *Frontiers in Immunology*, *13*(February), 1–12. https://doi.org/10.3389/fimmu.2022.823618

Marvel, D., & Gabrilovich, D. I. (2015). Myeloid-Derived Suppressor Cells in the Tumor Microenvironment: expect the unexpected. *The Journal of Clinical Investigation*, *125*(9). https://doi.org/10.1172/JCI80005

Mcinnes, L., Healy, J., & Melville, J. (2020). *UMAP: Uniform Manifold Approximation and Projection for Dimension Reduction*.

McLaughlin, J., Han, G., Schalper, K. A., Carvajal-Hausdorf, D., Pelakanou, V., Rehman, J., Velcheti, V., Herbst, R., LoRusso, P., & Rimm, D. L. (2016). Quantitative Assessment of the Heterogeneity of PD-L1 Expression in Non-small Cell Lung Cancer (NSCLC). *JAMA Oncology*, *2*(1), 46–54. https://doi.org/doi:10.1001/jamaoncol.2015.3638

Mechetner, E. B., Schott, B., Morse, B. S., Stein, W. D., Druley, T., Davis, K. A., Tsuruo, T., & Roninson, I. B. (1997). P-glycoprotein function involves conformational transitions detectable by differential immunoreactivity. *Proceedings of the National Academy of Sciences*, *94*(24), 12908–12913. https://doi.org/10.1073/pnas.94.24.12908

Movahedi, K., Guilliams, M., Van Den Bossche, J., Van Den Bergh, R., Gysemans, C., Beschin, A., De Baetselier, P., & Van Ginderachter, J. A. (2008). Identification of discrete tumor-induced myeloid-derived suppressor cell subpopulations with distinct T cell suppressive activity. *Blood*, *111*(8), 4233–4244. https://doi.org/10.1182/blood-2007-07-099226

Passiglia, F., Bronte, G., Bazan, V., Natoli, C., Rizzo, S., Galvano, A., Listì, A., Cicero, G., Rolfo, C., Santini, D., & Russo, A. (2016). PD-L1 expression as predictive biomarker in patients with NSCLC: A pooled analysis. *Oncotarget*, *7*(15), 19738–19747. https://doi.org/10.18632/oncotarget.7582

Patel, S. P., & Kurzrock, R. (2015). PD-L1 expression as a predictive biomarker in cancer immunotherapy. *Molecular Cancer Therapeutics*, *14*(4), 847–856. https://doi.org/10.1158/1535-7163.MCT-14-0983

Paver, E. C., Cooper, W. A., Colebatch, A. J., Ferguson, P. M., Hill, S. K., Lum, T., Shin, J. S., O'Toole, S., Anderson, L., Scolyer, R. A., & Gupta, R. (2021). Programmed death ligand-1 (PD-L1) as a predictive marker for immunotherapy in solid tumours: a guide to immunohistochemistry implementation and interpretation. *Pathology*, *53*(2), 141–156. https://doi.org/10.1016/j.pathol.2020.10.007

Paz-Ares, L. G., Ramalingam, S. S., Ciuleanu, T. E., Lee, J. S., Urban, L., Caro, R. B., Park, K., Sakai, H., Ohe, Y., Nishio, M., Audigier-Valette, C., Burgers, J. A., Pluzanski, A., Sangha, R., Gallardo, C., Takeda, M., Linardou, H., Lupinacci, L., Lee, K. H., … Reck, M. (2022). First-Line Nivolumab Plus Ipilimumab in Advanced NSCLC: 4-Year Outcomes From the Randomized, Open-Label, Phase 3 CheckMate 227 Part 1 Trial. *Journal of Thoracic Oncology*, *17*(2), 289–308. https://doi.org/10.1016/j.jtho.2021.09.010

Petriz, J., Bradford, J. A., & Ward, M. D. (2018). No lyse no wash flow cytometry for maximizing minimal sample preparation. *Methods*, *134–135*, 149–163. https://doi.org/10.1016/j.ymeth.2017.12.012

Pogoda, K., Pyszniak, M., Rybojad, P., & Tabarkiewicz, J. (2016). Monocytic myeloid-derived suppressor cells as a potent suppressor of tumor immunity in non-small cell lung cancer. *Oncology Letters*, *12*(6), 4785–4794. https://doi.org/10.3892/ol.2016.5273

Ratcliffe, M. J., Sharpe, A., Midha, A., Barker, C., Scott, M., Scorer, P., Al-Masri, H., Rebelatto, M. C., & Walker, J. (2017). Agreement between programmed cell death ligand-1 diagnostic assays across multiple protein expression cutoffs in non–small cell lung cancer. *Clinical Cancer Research*, *23*(14), 3585–3591. https://doi.org/10.1158/1078-0432.CCR-16-2375

Reck, M., Rodríguez-Abreu, D., Robinson, A. G., Hui, R., Csőszi, T., Fülöp, A., Gottfried, M., Peled, N., Tafreshi, A., Cuffe, S., O'Brien, M., Rao, S., Hotta, K., Leiby, M. A., Lubiniecki, G. M., Shentu, Y., Rangwala, R., & Brahmer, J. R. (2016). Pembrolizumab versus Chemotherapy for PD-L1–Positive Non–Small-Cell Lung Cancer. *New England Journal of Medicine*, *375*(19), 1823–1833. https://doi.org/10.1056/nejmoa1606774

Rehman, J. A., Han, G., Carvajal-Hausdorf, D. E., Wasserman, B. E., Pelekanou, V., Mani, N. L., McLaughlin, J., Schalper, K. A., & Rimm, D. L. (2017). Quantitative and pathologist-read comparison of the heterogeneity of programmed death-ligand 1 (PD-L1) expression in non-small cell lung cancer. *Modern Pathology*, *30*(3), 340–349. https://doi.org/10.1038/modpathol.2016.186

Rico, L. G., Aguilar Hernández, A., Ward, M. D., Bradford, J. A., Juncà, J., Rosell, R., & Petriz, J. (2021). Unmasking the expression of PD-L1 in Myeloid Derived Suppressor Cells: A case study in lung cancer to discover new drugs with specific on-target efficacy. *Translational Oncology*, *14*(1), 2020–2022. https://doi.org/10.1016/j.tranon.2020.100969

Rico, L. G., Salvia, R., Ward, M. D., Bradford, J. A., & Petriz, J. (2021). Flow-cytometry-based protocols for human blood/marrow immunophenotyping with minimal sample perturbation. *STAR Protocols*, *2*(4), 100883. https://doi.org/10.1016/j.xpro.2021.100883

Rimm, D. L., Han, G., Taube, J. M., Yi, E. S., Bridge, J. A., Flieder, D. B., Homer, R., West, W. W., Wu, H., Roden, A. C., Fujimoto, J., Yu, H., Anders, R., Kowalewski, A., Rivard, C., Rehman, J., Batenchuk, C., Burns, V., Hirsch, F. R., & Wistuba, I. I. (2017). A prospective, multi-institutional, pathologist-based assessment of 4 immunohistochemistry assays for PD-L1 expression in non–small cell lung cancer. *JAMA Oncology*, *3*(8), 1051–1058. https://doi.org/10.1001/jamaoncol.2017.0013

Scheel, A. H., Baenfer, G., Baretton, G., Dietel, M., Diezko, R., Henkel, T., Heukamp, L. C., Jasani, B., Jöhrens, K., Kirchner, T., Lasitschka, F., Petersen, I., Reu, S., Schildhaus, H. U., Schirmacher, P., Schwamborn, K., Sommer, U., Stoss, O., Tiemann, M., … Rüschoff, J. (2018). Interlaboratory concordance of PD-L1 immunohistochemistry for non-small-cell lung cancer. *Histopathology*, *72*(3), 449–459. https://doi.org/10.1111/his.13375

Scheel, A. H., Dietel, M., Heukamp, L. C., Jöhrens, K., Kirchner, T., Reu, S., Rüschoff, J., Schildhaus, H. U., Schirmacher, P., Tiemann, M., Warth, A., Weichert, W., Fischer, R. N., Wolf, J., & Buettner, R. (2016). Harmonized PD-L1 immunohistochemistry for pulmonary squamous-cell and adenocarcinomas. *Modern Pathology*, *29*(10), 1165–1172. https://doi.org/10.1038/modpathol.2016.117

Scheel, A. H., & Schäfer, S. C. (2018). Current PD-L1 immunohistochemistry for non-small cell lung cancer. *Journal of Thoracic Disease*, *10*(3), 1217–1219. https://doi.org/10.21037/jtd.2018.02.38

Skov, B. G., & Skov, T. (2017). Paired Comparison of PD-L1 Expression on Cytologic and Histologic Specimens from Malignancies in the Lung Assessed with PD-L1 IHC 28-8pharmDx and PD-L1 IHC 22C3pharmDx. *Applied Immunohistochemistry and Molecular Morphology*, *25*(7), 453–459. https://doi.org/10.1097/PAI.0000000000000540

Smith, J., Robida, M. D., Acosta, K., Vennapusa, B., Mistry, A., Martin, G., Yates, A., & Hnatyszyn, H. J. (2016). Quantitative and qualitative characterization of Two PD-L1 clones: SP263 and E1L3N. *Diagnostic Pathology*, *11*(1). https://doi.org/10.1186/s13000-016-0494-2

Sotillo, J., Cortés, A., Muñoz-Antoli, C., Fried, B., Esteban, J. G., & Toledo, R. (2014). The effect of glycosylation of antigens on the antibody responses against Echinostoma caproni (Trematoda: Echinostomatidae). *Parasitology*, *141*(10), 1333–1340. https://doi.org/10.1017/S0031182014000596

Szabó, Á., Szöllősi, J., & Nagy, P. (2022). Principles of Resonance Energy Transfer. *Current Protocols*, *2*(12). https://doi.org/10.1002/cpz1.625

Tian, X., Wang, T., Zheng, Q., Tao, Y., Dai, L., & Shen, H. (2021). Circulating CD15+LOX-1+ PMN-MDSCs are a potential biomarker for the early diagnosis of non-small-cell lung cancer. *International Journal of Clinical Practice*, *75*(8), 1–7. https://doi.org/10.1111/ijcp.14317

Tino, W. T., Huber, M. J., Lake, T. P., Greene, T. G., Murphy, G. P., & Holmes, E. H. (2000). Isolation and Characterization of Monoclonal Antibodies Specific for Protein Conformational Epitopes Present in Prostate-Specific Membrane Antigen (PSMA). In *HYBRIDOMA* (Vol. 19, Issue 3). Mary Ann Liebert, Inc. www.liebertpub.com

Vahedi, S., Lusvarghi, S., Pluchino, K., Shafrir, Y., Durell, S. R., Gottesman, M. M., & Ambudkar, S. V. (2018). Mapping discontinuous epitopes for MRK-16, UIC2 and 4E3 antibodies to extracellular loops 1 and 4 of human P-glycoprotein. *Scientific Reports*, *8*(1). https://doi.org/10.1038/s41598-018-30984-8

Van Der Maaten, L., & Hinton, G. (2008). Visualizing Data using t-SNE. *Journal of Machine Learning Research*, *9*, 2579–2605.

Van Gassen, S., Callebaut, B., Van Helden, M. J., Lambrecht, B. N., Demeester, P., Dhaene, T., & Saeys, Y. (2015). FlowSOM: Using self-organizing maps for visualization and interpretation of cytometry data. *Cytometry. Part A: The Journal of the International Society for Analytical Cytology*, *87*(7), 636–645. https://doi.org/10.1002/CYTO.A.22625

Woodford, R., Zhou, D., Lord, S. J., Marschner, I., Cooper, W. A., Lewis, C. R., John, T., Yang, J. C. H., & Lee, C. K. (2022). PD-L1 expression as a prognostic marker in patients treated with chemotherapy for metastatic non-small-cell lung cancer. *Future Oncology*, *18*(14), 1793–1799. https://doi.org/10.2217/fon-2021-1184

Xu, H., Lin, G., Huang, C., Zhu, W., Miao, Q., Fan, X., Wu, B., Zheng, X., Lin, X., Jiang, K., Hu, D., & Li, C. (2017). Assessment of Concordance between 22C3 and SP142 Immunohistochemistry Assays regarding PD-L1 Expression in Non-Small Cell Lung Cancer. *Scientific Reports*, *7*. https://doi.org/10.1038/s41598-017-17034-5

Yamauchi, Y., Safi, S., Blattner, C., Rathinasamy, A., Umansky, L., Juenger, S., Warth, A., Eichhorn, M., Muley, T., Herth, F. J. F., Dienemann, H., Platten, M., Beckhove, P., Utikal, J., Hoffmann, H., & Umansky, V. (2018). Circulating and tumor myeloid-derived suppressor cells in resectable non-small cell lung cancer. *American Journal of Respiratory and Critical Care Medicine*, *198*(6), 777–787. https://doi.org/10.1164/rccm.201708-1707OC

Yamazaki, T., Akiba, H., Iwai, H., Matsuda, H., Aoki, M., Tanno, Y., Shin, T., Tsuchiya, H., Pardoll, D. M., Okumura, K., Azuma, M., & Yagita, H. (2002). Expression of Programmed Death 1 Ligands by Murine T Cells and APC. *The Journal of Immunology*, *169*(10), 5538–5545. https://doi.org/10.4049/jimmunol.169.10.5538

Youn, J.-I., Nagaraj, S., Collazo, M., & Gabrilovich, D. I. (2008). Subsets of Myeloid-Derived Suppressor Cells in Tumor-Bearing Mice. *The Journal of Immunology*, *181*(8), 5791–5802. https://doi.org/10.4049/jimmunol.181.8.5791

Yue, C., Jiang, Y., Li, P., Wang, Y., Xue, J., Li, N., Li, D., Wang, R., Dang, Y., Hu, Z., Yang, Y., & Xu, J. (2018). Dynamic change of PD-L1 expression on circulating tumor cells in advanced solid tumor patients undergoing PD-1 blockade therapy. *OncoImmunology*, *7*(7), 1–12. https://doi.org/10.1080/2162402X.2018.1438111

Zahran, A. M., Hetta, H. F., Zahran, Z. A. M., Rashad, A., Rayan, A., Mohamed, D. O., Elhameed, Z. A. A., Khallaf, S. M., Batiha, G. E. S., Waheed, Y., Muhammad, K., & Nafady-Hego, H. (2021). Prognostic Role of Monocytic Myeloid-Derived Suppressor Cells in Advanced Non-Small-Cell Lung Cancer: Relation to Different Hematologic Indices. *Journal of Immunology Research*, *2021*. https://doi.org/10.1155/2021/3241150

Zak, K. M., Kitel, R., Przetocka, S., Golik, P., Guzik, K., Musielak, B., Dömling, A., Dubin, G., & Holak, T. A. (2015). Structure of the Complex of Human Programmed Death 1, PD-1, and Its Ligand PD-L1. *Structure*, *23*(12), 2341–2348. https://doi.org/10.1016/j.str.2015.09.010

Zhang, S., Ma, X., Zhu, C., Liu, L., Wang, G., & Yuan, X. (2016). The Role of Myeloid-Derived Suppressor Cells in Patients with Solid Tumors: A Meta-Analysis. *PLoS ONE*, *11*(10). https://doi.org/10.1371/journal.pone.0164514

FIGURES:

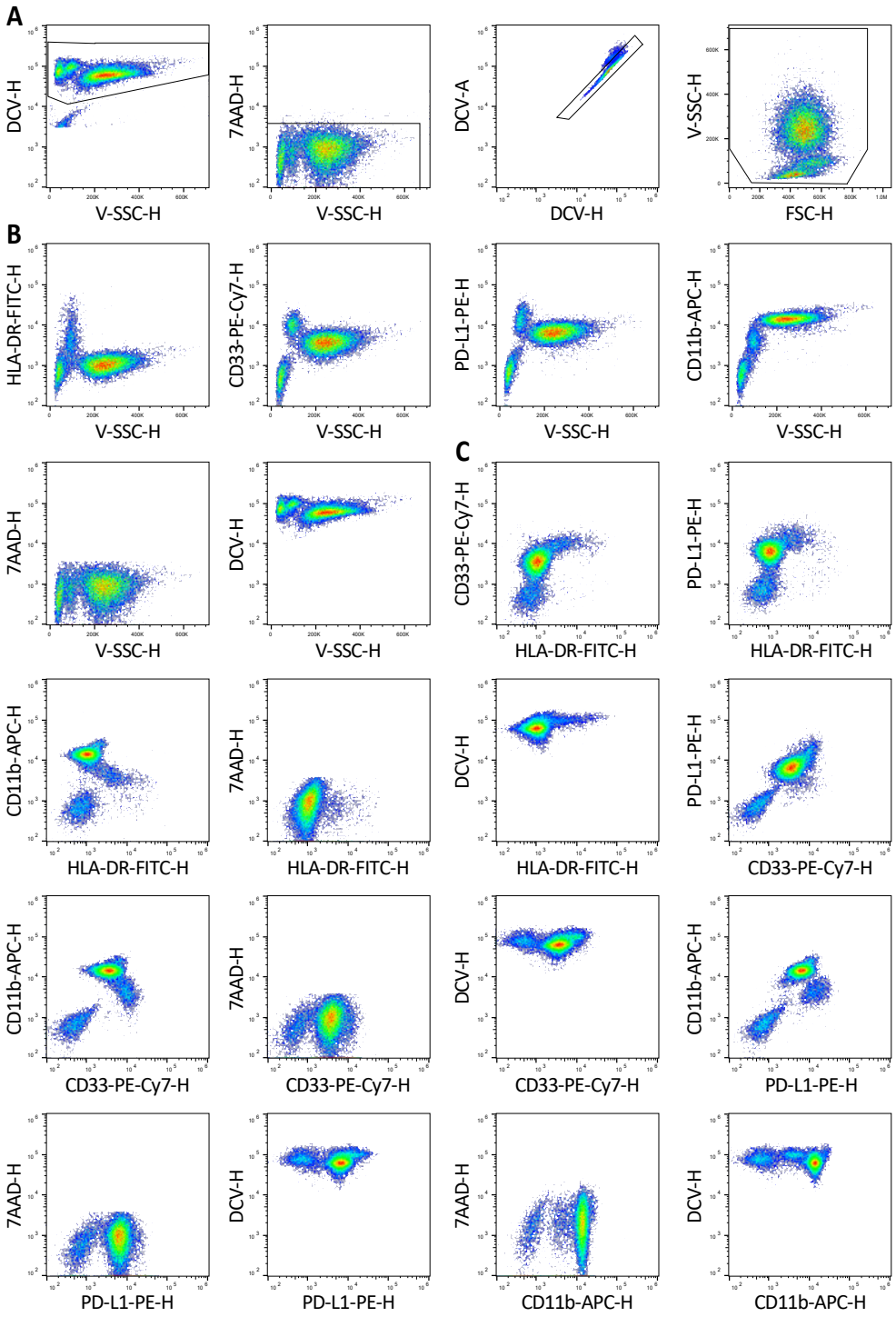

Figure 1. Flow cytometry panel for PD-L1⁺ MDSCs immunophenotyping. A) To visualize leukocytes, dual density plots are shown for the discrimination of non-nucleated cells, necrotic cells, doublets or aggregates. **B)** Dual density plots displaying each fluorochrome versus the violet scatter (V-SSC) are used to adjust the autofluorescence. **C)** Dual density plots combining all fluorochrome combinations for color compensation. FSC and V-SSC are set in linear scale, whereas fluorescence parameters are set in logarithmic scale.

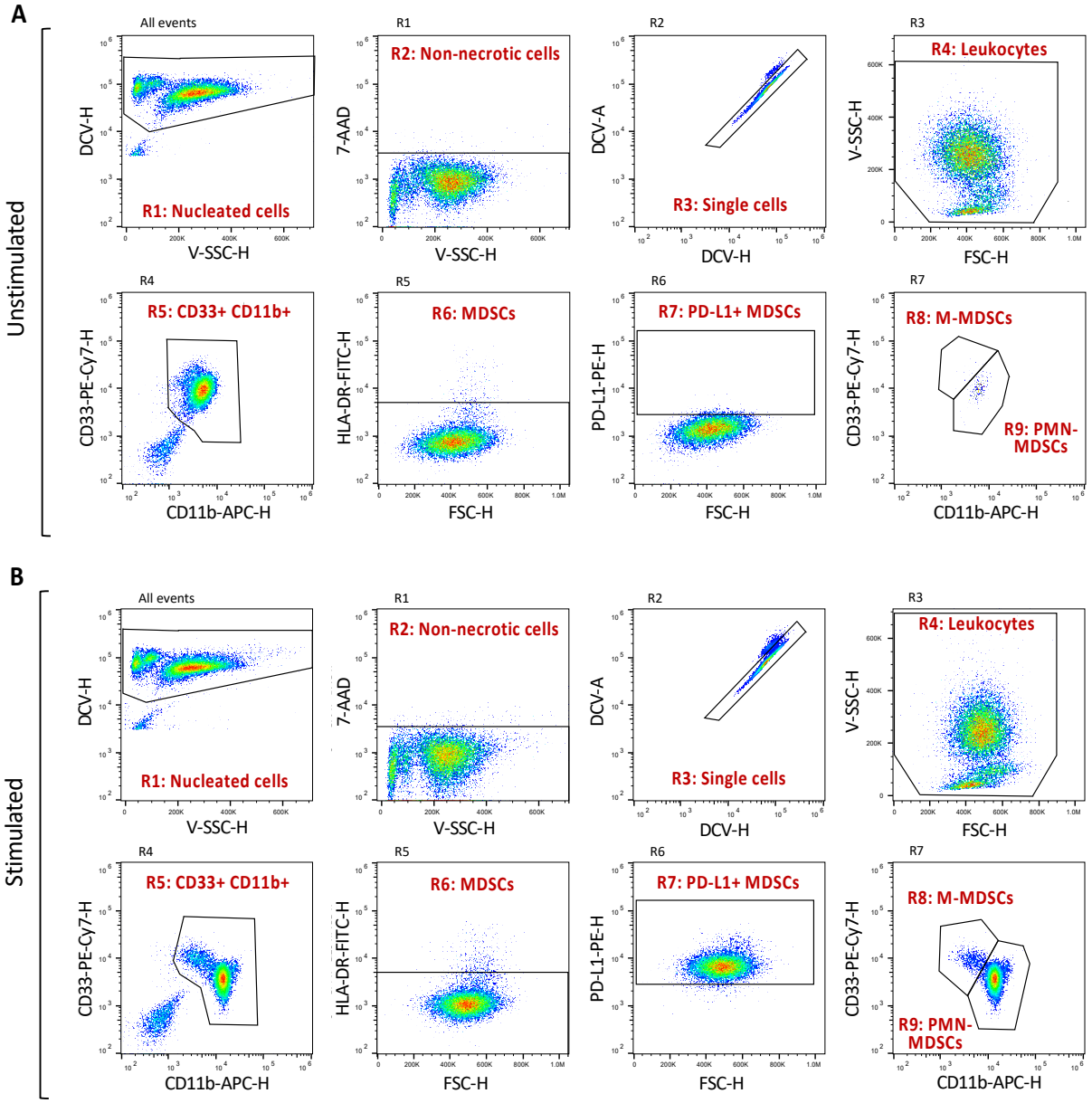

Figure 2. Flow cytometric acquisition strategy for MDSCs characterization and PD-L1 expression assessment. Representative peripheral blood sample analysis from a patient with NSCLC. First, the nucleated cells were selected with the DCV stain expression in R1, excluding erythrocytes, platelets, and debris. Then, the necrotic cells 7AAD+ were excluded from gate R2, and doublets and aggregates from R3 in a DNA-A vs DNA-H dual plot. Myeloid-derived suppressor cells were selected as $CD33^{+}$ $CD11b^{+}$ (R4) and HLA-$DR^{low/-}$ (R5). PD-$L1^{+}$ cells were selected in R6 and further subdivided in monocytic MDSCs (M-MDSCs) and polymorphonuclear MDSCs (PMN-MDSCs). A non-stimulated sample (DMSO) is shown on A and a stimulated sample (PMA) is shown on B. Samples were acquired using Attune™ NxT Flow Cytometer (Thermo Fisher) and analyzed in FlowJo™.

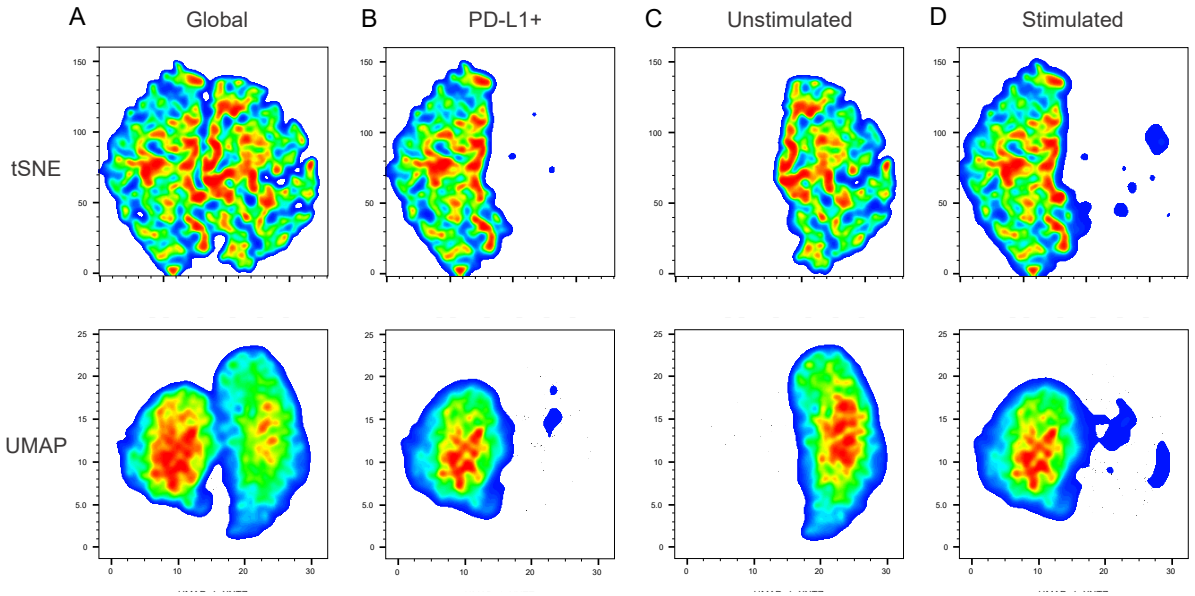

Figure 3. Representative t-SNE and UMAP analysis of MDSCs from non-small-cell lung cancer patients (n=20). t-SNE and UMAP analysis was performed on the myeloid-derived suppressor cell population, combining the following markers: CD33, CD11b, HLA-DR and PD-L1, and using the height (H) parameter. **A)** Global analysis of both stimulated and unstimulated MDSCs; **B)** PD-L1-expressing MDSCs; **C)** Unstimulated MDSCs, showing no PD-L1 reactivity; **D)** PMA stimulated MDSCs, showing PD-L1 reactivity.

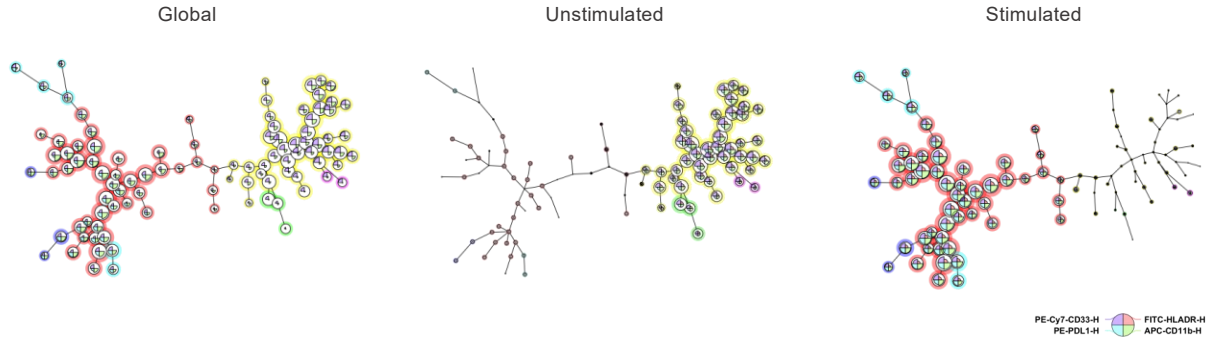

Figure 4. Representative FlowSOM analysis performed in a cohort of non-small-cell lung cancer patients (n=20). A global analysis was performed on the myeloid-derived suppressor cell population using the following markers: CD33, CD11b, HLA-DR and PD-L1. Plots from unstimulated and stimulated conditions were generated applying the global map structure, therefore maintaining the same disposition.

TABLES:

Table 1. Attune™ NxT Flow Cytometer configuration and labeling panel

Parameter	Laser	Detector	Pulse parameter	LP Filter	DLP Filter	BP Filter	Scale
FSC	488 nm	FSC	Height	Blank	555 nm	488/10 nm	Linear
Blue SSC	488 nm	SSC	Height	Blank	555 nm	488/10 nm	Linear
Violet SSC	405 nm	VL1	Height	Blank	495 nm	405/10 nm	Linear
DCV	405 nm	VL2	Height and Area	413 nm	495 nm	440/50 nm	Logarithmic
HLA-DR-FITC	488 nm	BL1	Height	496 nm	555 nm	530/30 nm	Logarithmic
7-AAD	488 nm	BL3	Height	496 nm	650 nm	695/70 nm	Logarithmic
PD-L1-PE	561 nm	YL1	Height	569 nm	600 nm	620/15 nm	Logarithmic
CD33-PE-Cy7	561 nm	YL4	Height	569 nm	740 nm	780/60 nm	Logarithmic
CD11b-APC	638 nm	RL1	Height	646 nm	690 nm	670/14 nm	Logarithmic

Table 2. Troubleshooting Guide for Basic Protocol 1: Sample preparation for PD-L1+ Myeloid-Derived Suppressor Cells detection by flow cytometry.

Problem	Possible Cause	Solution
Low signal	Fluorophore photobleaching	Cover the samples with aluminum foil to avoid light degradation
	Tandem dye degradation	Stain the samples with a new antibody vial. Minimize light exposure and temperature variations of the vial
	Antibody concentration is too low	Optimize antibody concentration with a titration curve
PD-L1 is not detected	Samples were not properly stimulated	Stimulate with PMA in a 37 °C water-dedicated bath for 5 min
	Antibody has different epitope reactivity and different affinity	Find suitable anti-PD-L1 (RUO or IVD)
	Sample manipulation: Lysing or trypsinization	Do not lyse the sample, follow minimal sample perturbation protocol Do not trypsinize adherent cells, use enzyme-free methods, such as scraping.
Positive population is not well separated from negative population	Unbound antibodies were not properly washed	Perform an additional wash step

High background	Sample degradation	Use freshly collected blood samples to avoid sample degradation
	Threshold is set on FSC or SSC	Set the threshold on the DNA-fluorescent probe to discriminate erythrocytes, platelets, and debris
Selective cell loss	Lysing and washing steps reduce cell numbers, especially neutrophiles	Avoid the use of lysing solutions by discriminating leukocytes with DNA-fluorescent probes

Table 3. Troubleshooting Guide for Basic Protocol 2: Protocol preparation, sample acquisition and gating strategy for flow cytometric screening of PD-L1^{+} Myeloid-Derived Suppressor Cells in Lung Cancer patients.

Problem	**Possible Cause**	**Solution**
No fluorescent signal from nucleated cells is detected	The laser and PMT settings are not compatible with fluorochrome / PMT voltage is too low for the fluorescent specific channel	Ensure that proper instrument settings are loaded prior to acquisition Use suitable positive and negative controls to optimize settings for every fluorochrome
	Increase or alternatively decrease fluorescence triggered throughput	Choose an appropriate threshold or thresholds to leave background out while selecting target cells Verify dye concentration, staining time, temperature and cell counting
	Background is too high	Dilute the sample to reduce background
Scattered light is not adequate to discriminate leukocytes	Sample rate is too high	Scatter degradation increases with event rate. Decrease sample rate or alternatively dilute the sample
	Pulse parameter use	Height (H) data is generally more accurate than area (A) data, owing to contributions in area from background coincidence
	Violet-SSC is in logarithmic scale	By default, VL1 is set in logarithmic scale. Change the scale into linear for scatter collection
High coincidence and low resolution	Running at a high flow rate can increase coincidence and lower resolution	Acoustic-assisted hydrodynamic focusing provided a more precise cell alignment, even at high flow rate. However, non-acoustic assisted hydrodynamic focusing cannot preserve the precision at a high flow rate when using whole blood samples. Whole blood samples should be run at medium/low flow rate

Table 4. Troubleshooting Guide for Support Protocol 2: Bioinformatic tools for the analysis of flow cytometric data.

Problem	Possible Cause	Solution
tSNE, UMAP or FlowSOM cannot run	The acquisition matrix differs among the flow cytometry files	Assign a suitable compensation matrix to normalize the compensation of all the files
	FCS files are modified or damaged	Export new FCS files
tSNE/UMAP analyses get blocked	The files contain too much information, and the algorithm cannot support the analysis	Downsize the number of events of each sample
		Concatenate the population of interest instead of the global events
Populations are not equally represented	The downsize is not performed properly because it is posteriorly applied on the concatenated file	In the concatenating wizard, assign a proper low number of events in order to concatenate the same number of events from every file
FlowSOM is tightly over-connected (Also applicable for UMAP and tSNE, though it is not that evident)	The self-organizing map is saturated with irrelevant information	Exclude markers and variables that do not add value to your analysis, such as FSC, SSC, and viability or necrotic markers
		Select one parameter pulse instead of the three of them (Area, Width and Height). Height is recommended because it is usually more accurate

Supplementary table 1. Spillover values of unstimulated and PMA-stimulated samples.

DMSO	BL1: HLA-DR-FITC	BL3: 7-AAD	YL4: CD33-PE-Cy7	YL1: PD-L1-PE	RL1: CD11b-APC	VL1: DCV
BL1: HLA-DR-FITC		0	0	0	0	0
BL3: 7-AAD	0		0	0	0	0
YL4: CD33-PE-Cy7	0	0		2.5	0	0
YL1: PD-L1-PE	0	0	0		0	0
RL1: CD11b-APC	0	0	0	0		0
VL1: DCV	0	0	0	0	0	

PMA	BL1: HLA-DR-FITC	BL3: 7-AAD	YL4: CD33-PE-Cy7	YL1: PD-L1-PE	RL1: CD11b-APC	VL1: DCV
BL1: HLA-DR-FITC		0	0	0	0	0
BL3: 7-AAD	0		0	0	0	0
YL4: CD33-PE-Cy7	0	0		5	0	0
YL1: PD-L1-PE	0	16	0		0	0
RL1: CD11b-APC	0	2	0	0		0
VL1: DCV	0	0	0	0	0	